Detection of vanadyl–nitrogen interaction in organs of the vanadyl-treated rat: electron spin echo envelope modulation study

Kouichi Fukui[a,*], Hiroaki Ohya-Nishiguchi[a], Masami Nakai[b], Hiromu Sakurai[b], Hitoshi Kamada[a]

[a]*Institute for Life Support Technology, Yamagata Technopolis Foundation, Numagi, Yamagata 990, Japan*
[b]*Department of Analytical and Bioinorganic Chemistry, Kyoto Pharmaceutical University, Yamashina-Ku, Kyoto 607, Japan*

Received 20 April 1995; revised version received 17 May 1995

Abstract ESEEM spectroscopy was applied for the first time to organs of an animal, viz. the kidney and liver of the rat treated with vanadyl sulfate. The aim of this study is to investigate the in vivo coordination structure of vanadyl ions administrated, and to gain information concerning the insulin-mimic activity of vanadium. ESEEM measurements for kidney and liver performed at 77 K have established nitrogen coordination to a certain percentage of vanadyl ion in the organs. The rotios of nitrogen-coordinating vanadyl ion were estimated as 70–80% in the liver, and 50–55% in the kidney. Isotropic portions of the ^{14}N HFC were estimated as $|A_{iso}|$~5.0 MHz for liver, and ~5.2 MHz for kidney, indicating that the coordinating nitrogen is an amino nitrogen. Coordination of the Lys ϵ-amine or the N-terminal α-amine of a protein or (a peptide) to vanadyl ion in vivo is suggested.

Key words: EPR; ESEEM; Vanadium; Diabetes; Insulin-mimic activity

1. Introduction

Vanadium ion has been reported to have an ability to mimic insulin activity. For example, it was reported that vanadate ion ($V^{V}O_4^{3-}$) enhances the glucose uptake [1,2], glycogen synthesis [3], and insulin-receptor kinase activity [4], and that doses of vanadate ion normalize the blood glucose level of the rat [5]. Vanadyl ($V^{IV}O^{2+}$) complexes were also examined and shown to have the same insulin-mimic activity [6,7]. These findings have aroused interests in the in vivo actions of vanadium. Vanadium is thought to act on peripheral cells, not on the insulin-releasing system, because no increase of the plasma insulin level was observed by administration of vanadium [5]. However the mechanism of the insulin-mimic activity of vanadium has not been revealed in spite of much effort. It was reported that vanadate peroxide system is more effective than vanadate alone and peroxide alone [8]. On the other side, however, reduction of vanadate ion to vanadyl ion under physiological conditions was also reported [1,6,9]. Sakurai et al. have shown that most of the dosed vanadium ions, even when the vanadium is furnished as vanadate ion, exist as vanadyl ion in organs [10]. Although it is still unclear whether the insulin-mimic activity comes from vanadyl or vanadate ion, the occurrence of reduction to vanadyl ion indicates that understanding of the in vivo coordination structure of vanadyl ions is crucial to reveal the mechanism of the insulin-mimic activity. It needs clarification whether administrated vanadyl ions are bound to certain proteins in vivo, and what the proteins are if this is the case.

In the present paper, we approach these questions by use of ESEEM spectroscopy. We applied for the first time ESEEM spectroscopy to organs of an animal, viz. the kidney and liver of the rat treated with vanadyl sulfate. It is known that administrated vanadyl ions distribute most in the kidney, followed by the liver [7c]. ESEEM spectroscopy can detect very weak hyperfine couplings (<20 MHz) which could not be observed by conventional CW EPR spectroscopy. Thus the nuclei with a non zero nuclear spin such as ^{1}H and ^{14}N may be detected. Preliminary measurements made for normal rats and STZ-induced diabetic rats showed no appreciable difference between their ESEEM's. Hence only the organs of normal rats were studied in detail. During the investigation, we have found that nitrogen coordination occurs for most vanadyl ions in the liver and more than half in the kidney. Thus we also investigated the ESEEM of vanadyl-histidine complex (VO-His) as a model of the vanadyl ions in the organs, and found that the ESEEM spectra of this complex are very similar to those of the organs. On the basis of this finding, the coordination environment of the nitrogen-coordinating vanadyl species in the organs is discussed.

2. Experimental

Wistar rats maintained on rat chow and weighing 190–210 g were induced diabetes by a single i.v. injection of freshly prepared STZ (60 mg/kg b.wt.) in 0.1 mM citrate buffer, pH 5.0. Both normal (mean serum glucose level for 2 animals, 135 mg/dl) and STZ-induced diabetic rats (mean serum glucose level for 2 animals, 419 mg/dl) were given daily i.v. injection of vanadyl sulfate (50 mg $VOSO_4 \cdot 6H_2O$/kg b.wt.), which corresponds to 9.3 mg vanadium/kg b.wt., in 0.9% (w/v) NaCl solution for four days. Serum glucose level of normal and STZ-induced rats treated with vanadyl sulfate were 111 mg/dl and 123 mg/dl, respectively. The kidneys and livers were removed from the rats, and cut into such pieces as can be put into a 5 mm φ EPR sample tube. Since preliminary ESEEM measurements for normal rats and STZ-induced diabetic rats showed no appreciable difference between their ESEEM's, detailed analysis was made only for the ESEEM's of normal rats. VO-His was measured in PBS (0.1 M phosphate buffer solution at pH 7.4)–ethyleneglycol glass (1:1 v/v).

CW EPR spectra were obtained on a Jeol RE-3X spectrometer with a low Q cavity designed for common use in CW and pulsed EPR measurements. ESEEM measurements were made on a Jeol RE-3X spectrometer and a JEOL ES-PX1000 pulse ESR unit, using two-pulse sequence ($\pi/2$–τ–π–τ–echo). The width for $\pi/2$ pulse was 15 ns, and τ was varied from 0.3 to 2.84 μs with 20 ns interval (128 data points). The two-pulse echo was found to almost disappear above ~2.5 μs. ESEEM

*Corresponding author. Fax: (81) (236) 47-3149.

Abbreviations: ESEEM, electron spin echo envelope modulation; CW EPR, continuous wave electron paramagnetic resonance; MEM, maximum entropy method; FT, Fourier transform; HFC, hyperfine coupling; NQC, nuclear quadrupole coupling; NZC, nuclear Zeeman coupling; STZ, streptozotocin.

SSDI 0014-5793(95)000595-1

data were collected on a Jeol Esprit 330 computer, and transformed into the frequency-domain spectrum with MEM. MEM is known to be more effective than Fourier transformation [11]. Computer simulation of ESEEM data were performed on the basis of the Mims equations [12].

3. Results

Fig. 1 shows the CW EPR spectrum for the kidney of the rat treated with vanadyl ion measured at 77 K. The CW EPR spectrum for liver (not shown) was almost identical with that for kidney except that the signal intensity was weaker owing to smaller vanadyl content in the liver [7]. Two-pulse ESEEM measurements were performed at three features of the CW EPR spectrum, as denoted as points A, B, and C in Fig. 1. Point A corresponds to the second parallel peak from low field. Unfortunately the first parallel peak from low field was very weak, and ESEEM measurements could not be made. Point B corresponds to the third perpendicular peak from low field, and point C corresponds to the composite of the fourth parallel and perpendicular peaks. The ESEEM spectra of kidney and liver are shown in Figs. 2 and 3, respectively. For both organs, intense peaks due to ^{1}H was observed (ν_H = 11.9, 13.0, 13.4 MHz at points A, B, and C, respectively), indicating the presence of water in the coordination sphere of vanadyl ions [13]. In some spectra, the ^{1}H peak appears as split. However, it is not clear whether this splitting is due to a real physical phenomenon or only an artifact formed in the generation of the MEM spectra [11]. Thus we did not analyze the ^{1}H signal further. The spectra exhibited other noticeable peaks in lower-frequency region. These peaks are attributed to ^{14}N. Therefore the ESEEM measurements have revealed that at least one nitrogen is coordinated to a certain amount of vanadyl ion in the organs. To our knowledge, this is the first direct evidence for the presence of vanadyl–nitrogen interaction in organs of an animal.

For comparison, we examined VO-His as a model of the nitrogen-coordinating vanadyl species in the organs. The ESEEM spectra of VO-His are presented in Fig. 4. The measurements were made at the CW EPR features corresponding to the points A, B, and C in Fig. 1. In the spectra, the ^{1}H signal appears at 11.9–13.4 MHz. The ^{1}H peaks were, however, weaker than those for the organs, which suggests that VO-His contains fewer water molecules in its coordination sphere. In the lower-frequency region, peaks attributable to ^{14}N were again observed. The frequencies and relative intensities of the

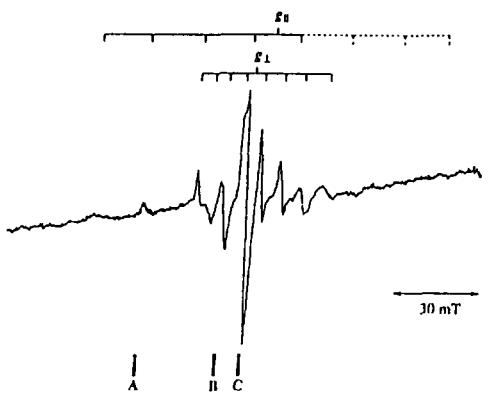

Fig. 1. CW EPR spectrum for the kidney of the rat treated with vanadyl ion (T = 77 K, ν = 8.86 GHz). ESEEM measurements were made at points A, B, and C.

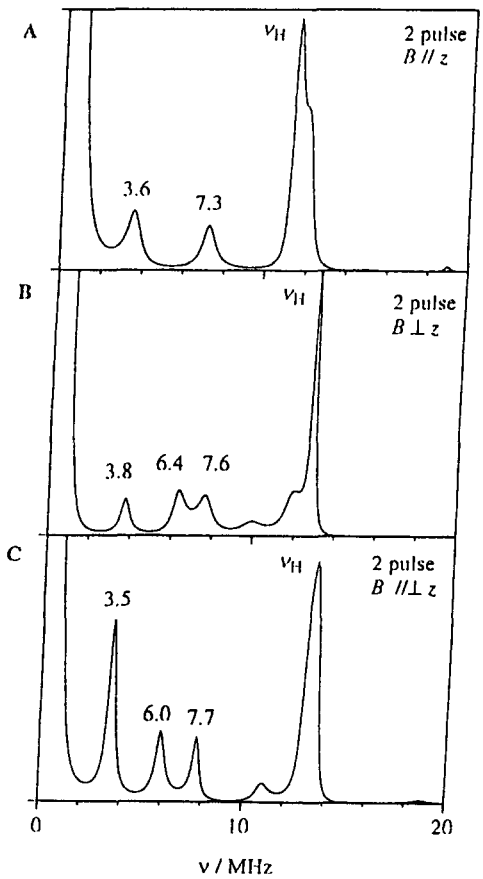

Fig. 2. Two-pulse ESEEM MEM power spectra for the kidney of the rat treated with vanadyl ion (T = 77 K, ν = 8.86 GHz). (A) B = 278 mT, $B//z$. (B) B = 305 mT, $B\perp z$. (C) B = 313 mT, $B//\perp z$.

^{14}N signals for VO-His are very similar to those for the organs. This similarity indicates that similar vanadyl-nitrogen interactions occur in VO-His and the nitrogen-coordinating species in the organs. (This does not necessarily mean histidine coordination to the vanadyl ion in the organs, vide infra.)

4. Discussion

4.1. Analysis of ESEEM

In all vanadyl complexes where the nitrogen atom is directly coordinated to the vanadyl ion, ^{14}N HFC is much stronger than ^{14}N NQC and NZC [14–18]. Under the condition of HFC ≫ NZC, NQC, the first-order perturbation theory provides the frequency of the ^{14}N ESEEM peaks as

$$\nu_{\pm} = A_p \pm 2\nu(^{14}N), \quad (1)$$

and

$$\nu_{\pm\pm} = A_p/2 \pm \nu(^{14}N) \pm 3Q_p/2, \quad (2)$$

where A_p and Q_p are the p components of HFC A and NQC Q tensors, respectively. The applied field is parallel to the p axis, and $\nu(^{14}N)$ is the Larmor frequency of the ^{14}N nuclear spin. The peaks $\nu_{\pm}$ derive from the double-quantum transitions, and $\nu_{\pm\pm}$ from the single-quantum transitions. The dou-

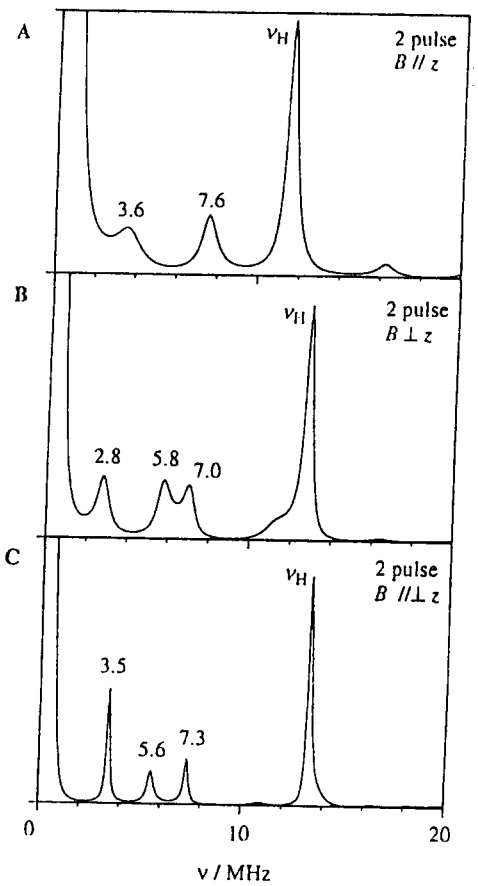

Fig. 3. Two-pulse ESEEM MEM power spectra for the liver of the rat treated with vanadyl ion (T = 77 K, ν = 8.86 GHz). (A) B = 279 mT, $B//z$. (B) B = 304 mT, $B\perp z$. (C) B = 312 mT, $B// \perp z$.

ble-quantum transition peaks are usually more intense than the single-quantum transition peaks in ESEEM in contrast to ENDOR spectroscopy. The single-quantum transition peaks will vanish when the electronic g, HFC A and NQC Q tensors are all coaxial (and the applied field is parallel to one of the principal axes of the coaxial tensors) [19].

When measurements are done at the parallel peak of the CW EPR spectrum, one observes single-crystal like spectra, where only the molecules whose g_z axis is parallel to the applied field are visible. Hence the interpretation of the spectra in Figs. 2A, 3A and 4A is straightforward. The pairs of ^{14}N peaks at ν = 3.6, 7.3 MHz for kidney, ν = 3.6, 7.6 MHz for liver, and ν = 3.2, 6.9 MHz for VO-His are assigned to the double-quantum transition peaks. The separations between the two peaks are 3.7, 4.0, and 3.7 MHz, respectively, which are comparable with the expected separation of $4\nu(^{14}N)$ = 3.4 MHz at B = 276 – 279 mT. The slight excess of the observed separation may be due to relatively low s/n of the observed ESEEM's [20]. From these assignments, one can estimate first-order approximate values of A_z = 5.5, 5.6, and 5.1 MHz for kidney, liver, and VO-His, respectively, using Eqn. 1. In the parallel spectrum of VO-His, an additional peak appears at ν = 5.2 MHz. We have assigned this peak to the ν_{++} peak, which gives Q_z = 1.2 MHz from Eqn. 2. As mentioned above, the single-quantum transition peaks gain intensity when the g, A, and Q tensors are not coaxial. The computer simulation including a slight deviation (ca. 5°) of the A_z and Q_z axes from the g_z axis well reproduced the observed spectrum (dotted line in Fig. 4A).

The ESEEM spectra obtained at the perpendicular peak exhibit the sum of the signals from the molecules whose g_z axis is perpendicular to the applied field. Therefore the interpretation of perpendicular spectra is not always straightforward. For the present case, however, the spectra (Figs. 2B, 3B, and 4B) can be interpreted in the same manner described above. The double-quantum transition peaks are assigned to the ν = 3.8, 7.6 MHz peaks for kidney, the ν = 2.8, 7.0 MHz peaks for liver, and the ν = 3.5, 6.8 MHz peaks for VO-His. The $A_{x,y}$ values are thus estimated as 5.7, 4.9, 5.2 MHz for kidney, liver, and VO-His, respectively, from Eqn. 1. The weak peak at 5.8 MHz for VO-His is assigned again to the x,y-averaged ν_{++} peak. The computer simulation supports these assignments (Fig. 4B). The 6.4 MHz peak for kidney and the 5.8 MHz peak for liver are also attributable to the ν_{++} peak. Probably the vanadyl ions in the organs are in more distorted coordination environment, and thus the ν_{++} peak gains more intensity than that of VO-His.

The results of computer simulation are summarized in Table 1 with previously reported results of nitrogen-containing vanadyl complexes. In the simulation, the splitting energies and

Table 1
ESEEM results of nitrogen-coordinating vanadyl ions

	HFC/MHz			NQC/MHz		Nitrogen type	Ref.
	$\lvert A_x\rvert$, $\lvert A_y\rvert$		$\lvert A_z\rvert$	e^2Qq	η		
VO^{2+} in kidney	$\lvert A_{iso}\rvert$ = 5.2						e
VO^{2+} in liver	$\lvert A_{iso}\rvert$ = 5.0						e
VO-His	4.4		5.0[d]	2.8	0.57[d]		e
$VO(Gly)_2$	4.85		5.3	2.55	0.5	amine	17
VO-PK-PEP[a]	4.8		5.1	2.55	0.5	Lys amine	17
E-VO-AdoMet-Tl[b]	5.2		5.5	3.0	0.3	AdoMet amine	18
$VO(hfac)_2$(imidazole)[c]	$\lvert A_{iso}\rvert$ = 7.6					imine	15
VO-transferrin	$\lvert A_{iso}\rvert$ = 6.6					His imine	15
VO-lactoferrin	$\lvert A_{iso}\rvert$ = 6.6					His imine	15
VO(OEP)	6.7	7.2	7.7	2.0	0.5	pyrrole	16

[a] PK = pyruvate kinase, PEP = phosphoenolpyruvate.
[b] E = *S*-adenosylmethionine synthase, AdoMet = *S*-adenosylmethionine.
[c] hfac = hexafluoroacetylacetanate.
[d] The g-axis frame and the A- and Q-axis frames are related by 5° rotation along the coaxial y-axis. Q_x = 1.4, Q_y = −0.3, Q_z = −1.1 MHz.
[e] This work.

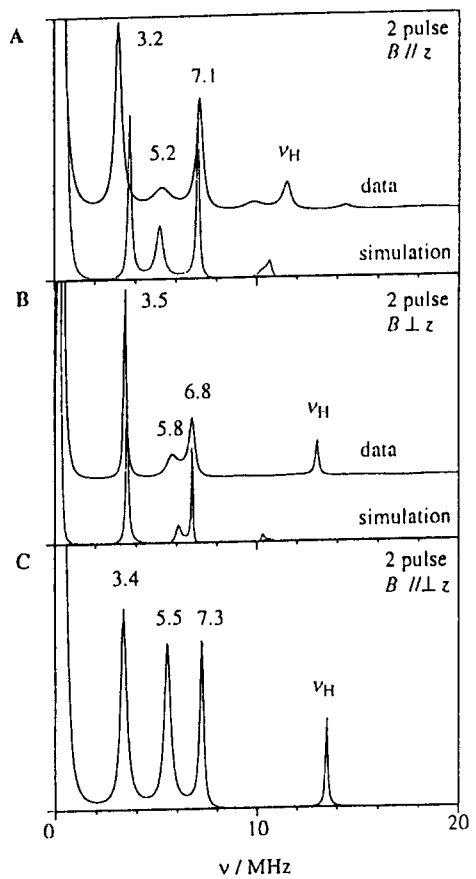

Fig. 4. Two-pulse ESEEM MEM power spectra of vanadyl-histidine complex in PBS-ethyleneglycol glass (1:1 v/v) (T = 77 K, ν = 8.86 GHz). Solid lines represent experimental data, and dotted lines represent simulations. (A) B = 276 mT, $B//z$. (B) B = 303 mT, $B \perp z$. (C) B = 312 mT, $B// \perp z$.

the peak intensities are computed through direct diagonalization of the spin Hamiltonian. Thus the obtained values are more reliable than the above values estimated from Eqns. 1 and 2. For VO-His, we have obtained satisfactory fits to the experimental data (dotted lines in Fig. 4). In the simulation, first we assumed that the g, A, and Q tensors are all coaxial. However, as described above, such simulations could not reproduce the ν = 5.2 MHz peak (in Fig. 4A) and ν = 5.8 MHz peak (in Fig. 4B). Hence we allowed non-coaxiality between the g and the other tensors (A_z and Q_z), where the A and Q tensors were still assumed as coaxial. The satisfactory fits shown in Fig. 4 have been achieved when the A_z and Q_z axes are taken as deviated by ca. 5° from the g_z axis (the A_x and Q_x axes are also deviated by ca. 5° from the g_x axis while the A_y and Q_y axes are still coincident with the g_y axis). In these simulations, we fixed as $A_x = A_y$. Further simulations allowing $A_x \neq A_y$ did not appreciably improve the fittings.

The simulations for the organs, unfortunately, did not give satisfactory fittings. Hence we present the current best where $A_x = A_y = A_z \equiv A_{iso}$ and the same Q tensor with that of VO-His are assumed. We attempted further simulations allowing free variation of these parameters, but the fitting was not improved appreciably. We suggest that the nitrogen-coordinating vanadyl species have several types. Between the types, nitrogen-coordination mode itself and/or combination with other ligands may be different.

4.2. Ratio of nitrogen-coordinating vanadyl ions

The coordination structures of the nitrogen-coordinating species in the organs and VO-His seem very similar. Thus we estimated the ratios of nitrogen-coordinating vanadyl ions by taking the ESEEM amplitude of VO-His as standard. We generated FT spectra [21] for the ESEEM's obtained at point C, and normalized the peak heights by their respective ν = 0 peak heights. The comparison between the normalized peak heights showed that the percentages of nitrogen-coordinating vanadyl ion are 50–55% for kidney and 70–80% for liver. These estimates indicate that the nitrogen-coordinating species are major ones especially in the liver.

4.3. Implications for the coordinating nitrogen in the organs

Table 1 indicates that vanadyl-nitrogen complexes can be divided into two categories according to their HFC parameters [14]: the first category comprises of imino- [14,15], and porphyrin pyrrole- [16] nitrogen coordinating complexes, where the A_{iso} values are in the range of 6–8 MHz. In the second category, amino nitrogens are coordinated to vanadyl ion [17,18], where the A_{iso} values distribute around 5 MHz (it seems that the imidazole nitrogen is not coordinated in VO-His). On the basis of this property of HFC parameter, we conclude that the coordinating nitrogen is an amino nitrogen. It is known that vanadyl ion form a complex with the imidazole nitrogen of His, the ε-amino nitrogen of Lys, and α-amino nitrogen of amino acids. Now we can exclude His imidazole nitrogen from the candidates of the coordinating nitrogen. Probably the ε-amine of Lys or the N-terminal α-amine of a protein (or a peptide) is coordinated to vanadyl ion.

In summary, the present ESEEM results strongly suggest formation of vanadyl-protein (or -peptide) complex in vivo. This supports the idea that administrated vanadyl ions are bound to proteins in vivo [9,22–24]. The ESEEM results also suggest that, in the vanadyl–protein (or -peptide) complex, the vanadyl ion is coordinated by the ε-amine of Lys or the N-terminal α-amine.

References

[1] Dubyak, G.R. and Kleinzeller, A. (1980) J. Biol. Chem. 255, 5306–5312.
[2] Miralpeix, M., Gil, J., Rosa, J.L., Carreras, J. and Bartrons, R. (1989) Life Sci. 44, 1491–1497.
[3] Tamura, S., Brown, T.A., Dubler, R.E. and Larner, J. (1983) Biochem. Biophys. Res. Commun. 113, 80–86.
[4] Tamura, S., Brown, T.A., Whipple, J.H., Fujita-Yamaguchi, Y. and Dubler, R.E. (1984) J. Biol. Chem. 259, 6650–6658.
[5] (a) Heylinger, C.E., Tahiliani, A.G. and McNeill, J.H. (1985) Science 227, 1474–1477. (b) Meyerovitch, J., Frafel, Z., Sack, J. and Shechter, Y. (1987) J. Biol. Chem. 262, 6658–6662.
[6] Shechter, Y. and Karlish, S.J.D. (1980) Nature 284, 556–558.
[7] (a) Ramanadham, S., Mongold, J.J., Brownsey, R.W., Cros, G.H. and McNeill, L.H. (1989) Am. J. Physiol. 257, 904–911; (b) Pederson, R. A., Ramanadham, S., Bucham, A.M.J. and McNeill, J.H. (1989) Diabetes 38, 1390–1395; (c) Sakurai, H., Tsuchiya, K., Nukatsuka, M., Sofue, M. and Kawada, J. (1990) J. Endocrinology 126, 451–459; (d) Sakurai, H., Tsuchiya, K., Nukatsuka, M., Sofue, M., Kawada, J., Ishikawa, S., Yoshida, H. and Komatsu, M. (1990) J. Clin. Biochem. Nutr. 8, 193–200; (e) Watanabe, H., Nakai, M., Komazawa, K. and Sakurai, H. (1994) J. Med. Chem. 38, 876–877.

[8] (a) Fantus, I.G., Kadota, S., Deragon, G., Foster, B. and Posner, B. I. (1987) Biochem. Biophys. Res. Commun. 147, 259–266; (b) Fantus, I.G., Kadota, S., Deragon, G., Foster, B. and Posner, B.I. (1989) Biochemistry 28, 8864–8871.
[9] Cantley Jr., L.C. and Aisen, P. (1979) J. Biol. Chem. 254, 1781–1784.
[10] Sakurai, H., Shimomura, S., Fukuzawa, K. and Ishizu, K. (1980) Biochem. Biophys. Res. Commun. 96, 293–298.
[11] (a) Stephenson, D.S. (1988) Progress in NMR Spectroscopy 20, 515–626; (b) Ormondt, D., V. and Nederveen, K. (1981) Chem. Phys. Lett. 82, 443–446.
[12] (a) Mims, W.B. (1972) Phys. Rev. B 5, 2409–2419; (b) (1972) Phys. Rev. 6, 3543–3545.
[13] Tyryshkin, A.M., Dikanov, S.A., Evelo, R.G. and Hoff, A.J. (1992) J. Chem. Phys. 97, 42–49.
[14] Tipton, P.A. and Peisach, J. (1991) Biochemistry 30, 739–744.
[15] Eaton, S.S., Dubach, J., More, K.M., Eaton, G.R., Thurman, G. and Ambruso, D.R. (1989) J. Biol. Chem. 264, 4776–4781.
[16] Fukui, K., Ohya-Nishiguchi, H. and Kamada, H. (1993) J. Phys. Chem. 97, 11858–11860.
[17] Tipton, P.A., McCracken, J., Cornelius, J.B. and Peisach, J. (1989) Biochemistry 28, 5720–5728.
[18] Zhang, C., Markham, G.D. and LoBrutto, R. (1993) Biochemistry 32, 9866–9873.
[19] Flanagan, H.L. and Singel, D.J. (1987) J. Chem. Phys. 87, 5606–5616.
[20] MEM seeks for the power spectrum $p(\nu)$ which has a maximum entropy $S = \int \ln p(\nu) d\nu$ from the $p(\nu)$'s consistent with given time-domain data. In general, a smoother spectrum has a larger entropy, and thus MEM spectra usually have smooth baselines regardless of noise level in time-domain data. It seems that the influence of noise appears rather as broadening of peaks and shift of peak positions.
[21] One important defect of MEM is that the spectral peak heights may not be correct: some peaks may be enhanced, or some peaks may be depressed from the true heights. Hence, in estimating the ratio, we used Fourier transformation in order to avoid this problem.
[22] Nakai, M., Watanabe, H., Fujiwara, C., Kakegawa, H., Satoh, T., Takeda, J., Matsushita, R. and Sakurai, H. (1995) Biol. Pharm. Bull. 18, 719–725.
[23] Cantley, Jr, L.C., Resh, M.D. and Guidotti, G. (1978) Nature 272, 552–554.
[24] Crans, D.C., Bunch, R.L. and Theisen, L.A. (1989) J. Am. Chem. Soc. 111, 7597–7607.